Plasmonic Op-Amp Circuit Model using the Inline Successive Microring Pumping Technique

P. Youplao[1], N. Sarapat[2], N. Porsuwancharoen[1], K. Chaiwong[3], M.A. Jalil[4] I.S. Amiri[5], J. Ali[6], M.S. Aziz[6], S. Chiangga[7], G. Singh[8], P. Yupapin[9, 10*], and K.T.V. Grattan[11]

[1]Department of Electronics Engineering, Faculty of Industry and Technology,
Rajamangala University of Technology Isan, Sakon Nakhon Campus, Sakon Nakhon, 47160, Thailand;
[2]Faculty of Science and Technology, Thepsatri Rajabhat University, Lopburi, 15000, Thailand;
[3]Faculty of Industrial Technology, Leoi Rajabhat University, Leoi 42000, Thailand;
[4] Department of Physics, Faculty of Science, Universiti Teknologi Malaysia, 81310 Johor Bahru Malaysia,
81300 Johor Bahru, Malaysia;
[5]Division of Materials Science and Engineering, Boston University, Boston, MA, 02215, USA;
[6] Laser Center, IbnuSina Institute for Industrial and Scientific Research, UniversitiTeknologi Malaysia (UTM)
[7]Department of Physics, Faculty of Science, Kasetsart University, Bangkok 10900, Thailand;
[8]Department of Electronics and Communication Engineering, Malaviya National Institute of Technology Jaipur, 302017, India;
[9]Computational Optics Research Group, Advanced Institute of Materials Science, Ton Duc Thang University,
District 7, Ho Chi Minh City, 700,000, Vietnam;
[10]Faculty of Electrical & Electronics Engineering; Ton Duc Thang University, District 7,
Ho Chi Minh City, 700,000, Vietnam;
[11]Department of Electrical & Electronic Engineering, School of Mathematics, Computer Science & Engineering, City,
University of London, London, EC1V 0HB, United Kingdom;
*Corresponding author E-mail:preecha.yupapin@tdt.edu.vn

Abstract: The electro-optic power pumping system model using the inline successive technique within the modified add-drop filter is proposed. A pumping system consists of a closed loop panda ring resonator, from which the optical power is coupled inline into the system. By controlling the two side phase modulators, the whispering gallery mode (WGM) is generated by the amplitude-squeezed light within the modified add-drop filter. By using the proposed circuits, the low current can be applied into the system via a gold layer connection, from which the amplified output current can be obtained at the throughput port, which can be functioned as the electronic operational amplifier (Op-amp). In application, the WGM output is the amplified signal that can be used for the up (down) link in free space communication network called light fidelity (LiFi). The electro-optic signals conversion can be performed by the stacked layers of silicon-graphene-gold materials. The results obtained have shown that large gain is obtained at the WGM output, which is $\sim 5 \times 10^{-6} cm^2.(V.sW)^{-1}$, when the pumping saturation time is ~2 fs. It concludes the suitability of our proposed model for light fidelity, LiFi up-down link conversion.

Keywords: MEMS/NEMS; MZI; Optical pumping; Microring resonator; Successive pumping;

1. Introduction

An optical repeater is the most important equipment in the optical transmission line and networks. There are many types of repeaters available nowadays [1-4], where the trends of the optical devices and components are focused on the small scale device regime that can have the system redundancy in terms of size and system performance, especially, the transmission capacity [5-8]. Pornsuwancharoen et al have shown a promising form of the material called a plasmonic island, which consists of the stacked layers of silicon-grapheme-gold materials [9-12]. They have reported that the electro-optic signal conversion can be carried out within the micro-scale device. The advantage of the system is that the output of the modified add-drop filter (panda ring) can be generated in the form of the WGM output. This can provide the use of free space link named as light fidelity (LiFi), where the broadband up and down links are required for the large demands of users [13-17]. WGM of light generated by the small-scale devices has been widely investigated and used [18-23]. One of them is the WGM generated by the microring resonator [9], which shows the potential for the light source, energy source, and sensor application. This paper presents the use of a closed loop panda ring resonator for the optical power pumping that has, to the best of our knowledge, never been presented elsewhere because of the conflict of interest with the energy conservation concept. Recently, we have found that this problem is clearly understood by using the squeezed monochromatic light within a microring resonator, where light pulse (photon) is projected by the quantum harmonic oscillator [24], in which light can be squeezed and observed under specific conditions. The uncertain saturation in terms of $\Delta E \Delta t$ or $\Delta X \Delta P$ has shown interesting results when the monochromatic light propagates within the nonlinear microring resonator, where the limitation of the energy conservation and the uncertainty saturation can give rise to useful applications. By using the squeezing concept, the inline and successive pumping systems can be employed within the optical transmission link that can be used for optical power recovery [25-27]. In this work, the inline and successive pumping schemes are combined together, in which the electrical current amplifier and optical power pumping can be employed. The equipment such as electro-optical power charger, multiplexer, modulator and filter can also be applied. The simulations are performed using the Opti-wave and MATLAB programs, and obtained the pumping output characteristics and the saturation times which are potentially usable for practical applications. Theoretical background of the presented investigation is given below.

2. Background

The inline coupled power from the monochromatic light source is input into the system as shown in Figure 1, which can be controlled by the selected coupling length (or gap). By controlling the two side ring radii, WGM output, which is the electrical field output (E_{PI}), can be obtained according to relation given in Eq 1 [19].

$$\boldsymbol{E_{PI}(\rho,\varphi)} = \frac{4\pi\,\mathrm{cosech}\left(k_{0n}\frac{\pi a}{2}\right)}{a^2 J_1^2(k_{0n}a)}\left[\frac{x_1\sqrt{k_1}}{\sqrt{1-2x_1y_1cos(k_nL)+e^{-\alpha L}x_1^2y_1^2}}\right]\cdot\frac{(wA_0)\sqrt{k_0n_0}}{B^{\frac{1}{4}}}J_0(k_{0n}\rho)\int_0^a J_0(k_{0n}\rho)\left[\rho-\left(\frac{A}{2(B+C\rho^2)}+\frac{C}{4B}\right)\rho^3\right]d\rho \quad (1)$$

Equation (1) is the electrical field in the cylindrical coordinate, where $A = k_{mn}^2 k_0^2 w^2 n_0^2 \rho^2$, $B = w^4 k_0^2 n_0^2$, $C = \varphi^2$, w, A_0 is constant of input signal, a is the radius of center ring, $x_1 = \sqrt{1-\gamma_1}$, $y_1 = \sqrt{1-\kappa_1}$, n_0 = linear refractive index, $k_0 = \frac{2\pi}{\lambda_0} n_{eff}$, n_{eff} is effective index, λ_0 is input wavelength, ρ and φ are the cylindrical coordinate radius and phase respectively, κ_1, γ_1 is the coupling constant and attenuation coefficient between linear waveguide and center of Panda ring resonator, k_{0n} is the wave number in the Bessel's function (J_0) by n is mode of electromagnetic field, and L is the center ring circumference.

For simplicity, the graphical method (Optiwave program) is utilized, from which the required outputs such as WGM and E_{th} are obtained. By using the equations (1)-(3), the optical input field (E_{in}) and output field (E_{th}) of the closed loop Panda ring system as shown in Figure 1 are obtained. More details are found in the reference [6].

$$\boldsymbol{E_{in}} = \boldsymbol{E_Z} = \boldsymbol{E_0 e^{-ik_z t-\omega t}} \quad (2)$$

$$\boldsymbol{E_{th}} = \bar{A}\boldsymbol{E_{in1}} - \bar{B}\boldsymbol{E_{in2}} e^{\frac{-\alpha L}{2\,2}-jk_n\frac{L}{2}}\left[\frac{\bar{C}E_{in1}\left(e^{\frac{-\alpha L}{2\,2}-jk_n\frac{L}{2}}\right)^2+\bar{D}E_{in2}\left(e^{\frac{-\alpha L}{2\,2}-jk_n\frac{L}{2}}\right)^3}{1-\bar{F}\left(e^{\frac{-\alpha L}{2\,2}-jk_n\frac{L}{2}}\right)^2}\right] \quad (3)$$

Where E_0 is the electric field amplitude (real), $\boldsymbol{k_z}$ is the wave number in the propagation direction, $\boldsymbol{\omega}$ is the angular frequency, t is the time evolution. E_{in1} and E_{in2} are the input at the input and control(add) ports respectively. α is the attenuation coefficient. $x_2 = \sqrt{1-\gamma_2}, y_2 = \sqrt{1-\kappa_2}$, $\bar{A} = x_1x_2, \bar{B} = x_1x_2y_2\sqrt{\kappa_1}E_{0L}$, $\bar{C} = x_1^2x_2\kappa_1\sqrt{\kappa_2}E_{0r}E_{0L}$, $\bar{D} = (x_1x_2)^2y_1y_2\sqrt{\kappa_1\kappa_2}E_{0r}E_{0L}^2$, $\bar{F} = x_1x_2y_1y_2E_{0r}E_{0L}$. E_{0r} and E_{0L} are the optical fields circulated components of the right and left hand phase modulators.

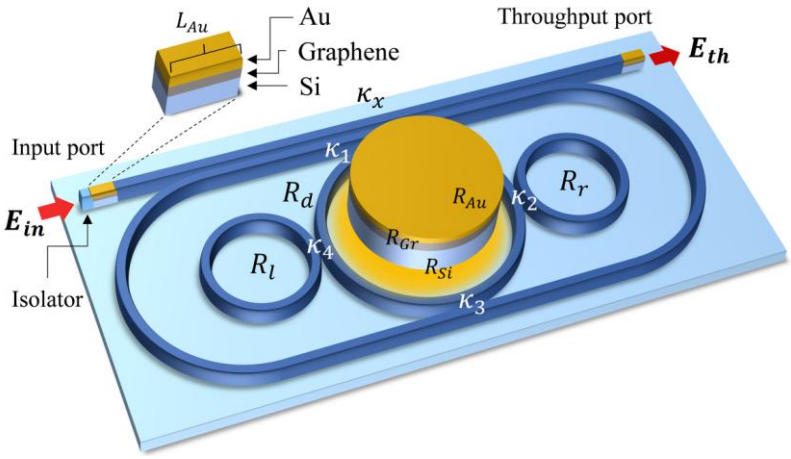

Figure 1: A schematic illustration of a closed loop Panda-ring for the inline successive pumping, where R_d, R_r, R_l,are the ring radii of the center ring and two side rings, right (R_r) and left (R_l) hands, R_{Si}: Silicon ring radius, R_{Gr}: Graphene ring radius, R_{Au}: Gold ring radius. E_{in} and E_{th} are the input and throughput electrical fields, respectively. The coupling constants $\kappa_1 = \kappa_2 = \kappa_3 = \kappa_4 = 0.5$.

3. Simulation Results

Under specific conditions, the throughput port output can be observed due to resonant condition, however, the energy conservation of the system must be satisfied, hence, the normalized system is applied for the remaining power. Additionally, the squeezed light saturation has also taken part to maintain the pumping system validation. The optical power of inline input optical field (E_{in}) is coupled into the closed loop Panda-ring system via the selected gap as shown in Figure 1 A fraction of this power is coupled into the Panda-ring system and into the add port respectively. Hence, the add port optical power becomes the input power of the successive system. Similarly, the fraction power from the add port is coupled into the system and into the drop port of the closed loop microring system. Finally, the drop port output is entered into the input port, from which the closed loop circulation is completed. The process repeats until the system achieves the resonant condition, where the pumping power output is saturated. The desired optical output is the WGM that can be obtained by adjusting the two side ring parameters. By using the plasmonic island, the electron mobility within the plasmonic island is driven by the WGM output, which is the driven group velocity. The required out is the resonance that can be obtained when the output mobility is saturated and the successive pumping time is known.

In simulation, a fraction of the transmission line power is coupled into the successive pumping system where the input source wavelength is 1.55 µm. The advantage of the modified add-drop filter with two side rings is that the nonlinear effect can offer shorter output pulse width and easier WGM resonant output control than the tradition system. Moreover, the pumping power can be squeezed and used for uplink transmission. The reversed direction (downlink) can also be applied by connecting with the plasmonic island. The successive pumping is performed and the required resonant output is obtained and plotted. Other simulation parameters are given in the figure captions and the following contents. In Figure 1, the resonant pumping output is the WGM output of the equation (1) [19]. It is the driven group velocity that can escalate the electron mobility. The relationship between the light intensity (I), group velocity and the electron mobility can be expressed as $\boldsymbol{I = E^2 = (\frac{V_d}{\mu})^2}$, which is defined by $V_d = \mu E$. When an electric field E is applied to the grating sensor, an electric current is established in the conductor. The density J_s of this current is given by $J_s = \sigma E$. The constant of proportionality σ is called the specific conductance or electrical conductivity of the conductor, for gold it is 1.6×10^8 $W^{-1}m^{-1}$ [28, 29]. The electron mobility in gold is 42.6 $cm^2 V^{-1} s^{-1}$, the electron mass is 9.10×10^{-31} kilograms, the electron charge is 1.60×10^{-19} coulombs. The refractive index of the silicon is 1.46. The linear and nonlinear refractive indices of the GaAsInP/P are 3.14 and 1.30×10^{-13} m^2W^{-1}, respectively. The attenuation coefficient of the waveguide is 0.1 dB $(mm)^{-1}$. In simulation, the input power from the remote source is coupled into the island via the coupling lens. The input power was varied from 0.5-5.0 W. By using the graphical method (Opti-wave), the simulation results are as shown in Figure 2, in which the required pumping is done by WGM. Selected parameters are then used for simulation with MATLAB program. The plot of the relationship between the input power and the output driven mobility is sown in Figure 3, which is showing promising results. The plot of the input, through port and island outputs is shown in Figure 3(a), (b) and (c) respectively, the large output gain is obtained at the WGM output, which is $\sim 5 \times 10^{-6} cm^2.(V.sW)^{-1}$. The output mobility is plotted against the pumping time as shown in Figure 4, which gives the output mobility of $\sim 5 \times 10^{-6} cm^2.(V.s)^{-1}$ for a pumping time of ~2 fs and input power of 1.0-5.0 W. From these results, it is shown that the use of the proposed system for a plasmonic op-amp and an up-downlink is possible, especially, for LiFi (free space) link.

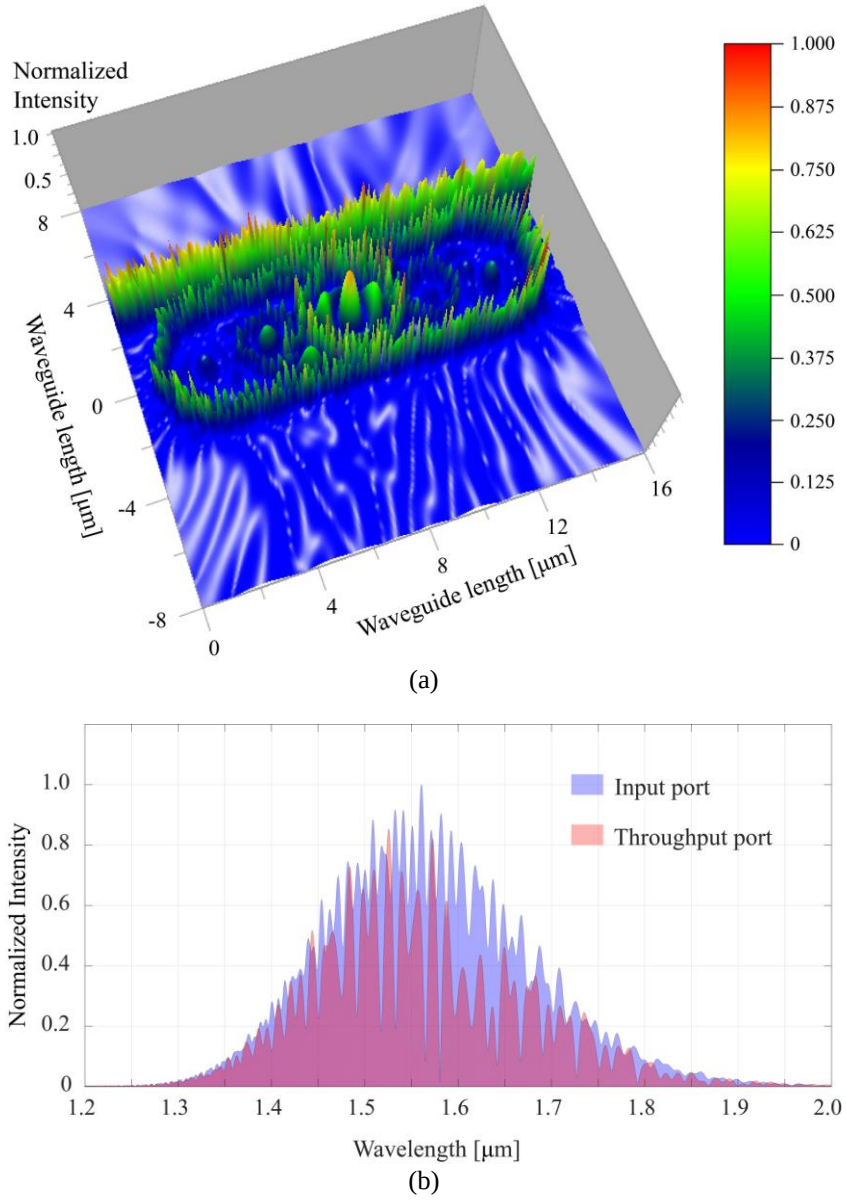

Figure 2: Shows (a) the 3D Opti-wave result of the system in Figure 1 for preliminary investigation, the parameters are the input power = 1.0 W, R_d = 1.6 µm, $R_l = R_r$ = 0.9 µm, $R_{Si} = R_{Gr} = R_{Au}$ = 1.5 µm, (b) input and throughput port signals.

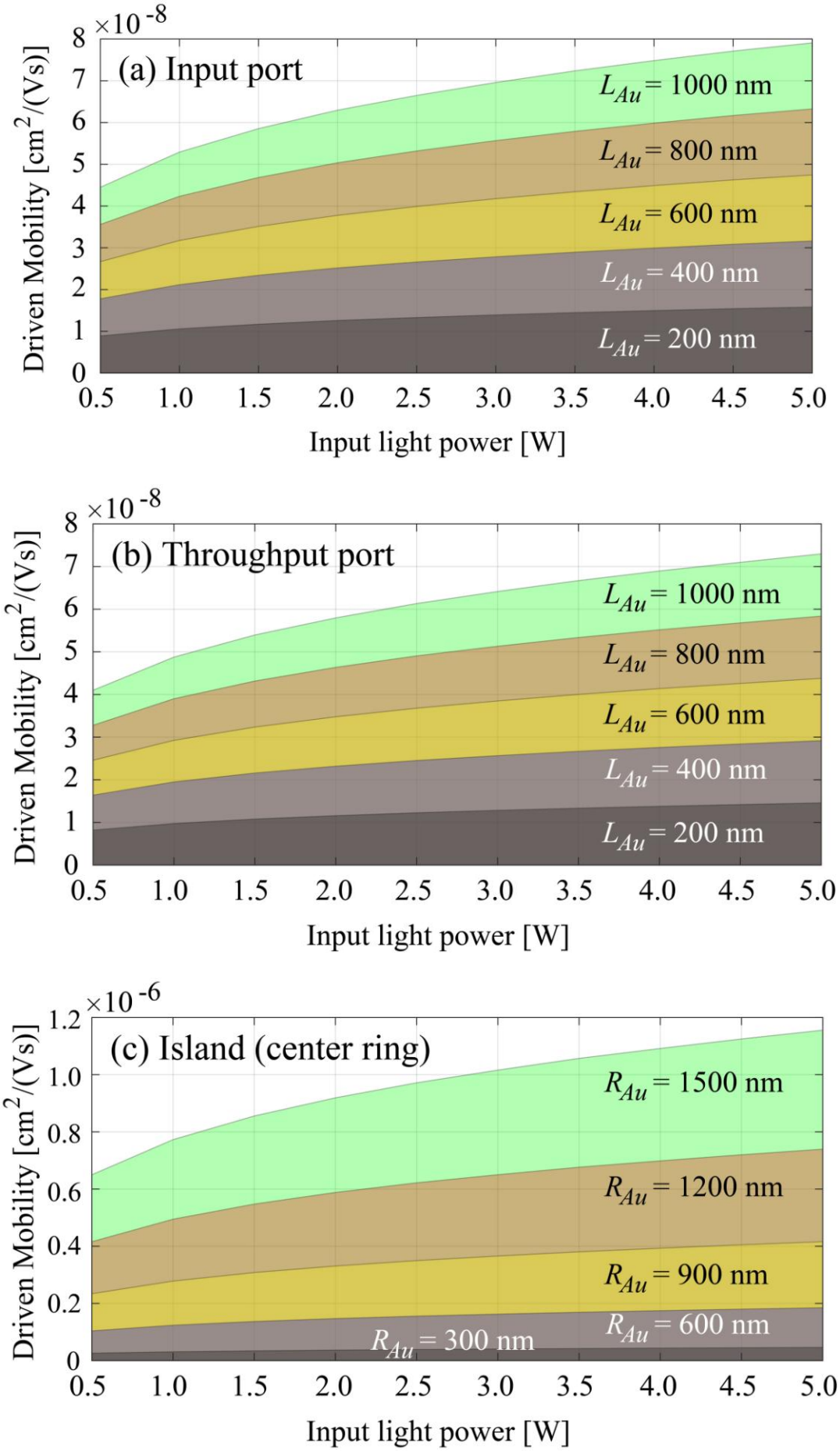

Figure 3: The plots of the mobility outputs, the gold and graphene layer parameters are w = 0.5 μm, thickness = 0.5 μm, the gold and graphene island thickness = 0.5 μm.

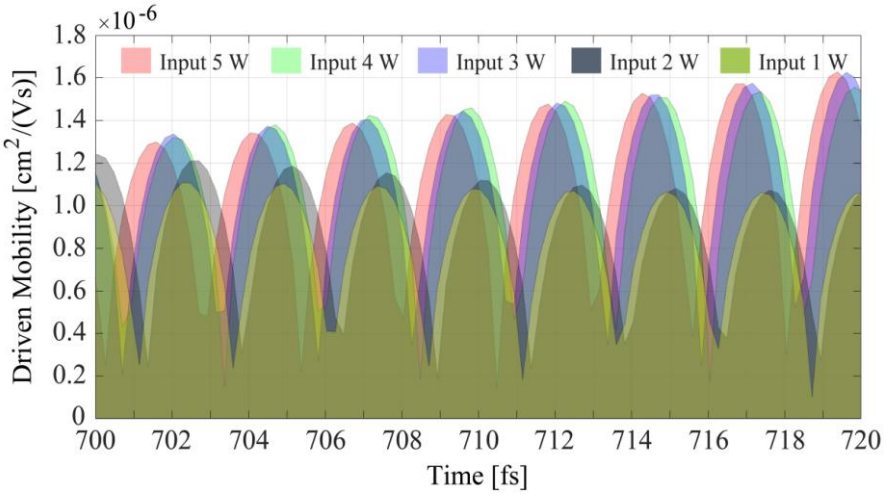

Figure 4: The plot of the mobility output of the plasmonic island with time for various input coupling power. The gold and graphene island parameters are thickness = 0.5 µm, $R_{Si} = R_{Gr} = R_{Au}$ = 1.5 µm, the input light power are ranged from 1 W to 5 W.

4. Conclusion

We have shown that the optical power inline pumping using the closed loop Panda-ring for up-downlink conversion, especially, for LiFi network. Since large bandwidth (high bit rate) can be obtained with LIFI it can accommodate large demands of users in terms of information capacity. Moreover, the free space transmission can provide the light power that can be used for other purposes, for instance, a remote charger and the internet of things (IoT) applications. In this article, we have modeled the LiFi up-down link node using the plasmonic island embedded within the closed loop Panda-ring system. By using the selected parameters obtained from the graphical method (Opti-wave program), the simulations have shown promising results. By using the MATLAB program, the results obtained show that the mobility of the WGM output is $\sim$5 x $10^{-6} cm^2.(V.sW)^{-1}$. The up-down converter link time of $\sim$2 fs is achieved after the inline successive pumping power is saturated. By using the throughput port output, the use of such a proposed system for a plasmonic op-amp is also possible.

Acknowledgments

The authors would like to give the appreciation for the research financial support by GUP project (Tier2 15J57) and Flagship UTM Shine Project (03G82) to the Universiti Teknologi Malaysia, Johor Bahru, Malaysia.

References

[1] Elkouss, D., Mateo, J.M., Ciurana, A., Martin, V. 2013, Secure optical networks based on quantum key distribution and weakly trusted repeaters, IEEE/OSA Journal of Optical Communications and Networking, 5(4), 316-318.

[2] Chan, C.A., Attygalle, M., Nirmalathas, A. 2010, Remote repeater-based EPON with MAC forwarding for long-reach and high-split-ratio passive optical networks, IEEE/OSA Journal of Optical Communications and Networking, 2(1), 28-37.

[3] Aida, K. and Amemiya, M. 1984, Undersea transmission-system reliability with laser-diode standby-redundant optical repeaters, IEEE Transaction on Reliability, R-33(5), 439-441.

[4] Nadarajah, N., Chae, C.-J., Tran, A.V., Nirmalathas, A. 2009, Optical layer local area network emulation in a multifunctional repeater-based optical access network, IEEE/OSA Journal of Optical Communications and Networking, 1(1), 43-49.

[5] Bogaerts, W., Heyn, P.D., Vaerenbergh, T.V., Vos, K.D., Selvaraja, S.K., Claes, T., Dumon, P., Bienstman, P., D. V. Thourhout, and R. Baets. 2012, Silicon Microring Resonators, Laser Photonics Rev., 6(1), 47-73.

[6] Amiri, I.S., Ali, J. and Yupapin, P.P. 2012, Enhancement of FSR and finesse using add/drop filter and panda ring resonator, J. Mod. Phys. B 26, 1250034.

[7] Phatharaworamet, T., Teeka, C., Jomtarak, R., Mitatha, S. and Yupapin, P.P., 2010. Random binary code generation using dark-bright soliton conversion control within a Panda Ring resonator, J Lighwave Technol., 28(19), 2804-2809.

[8] S. Mitatha, N. Pornsuwancharoen, P.P. Yupapin. 2009, A simultaneous short-wave and millimeter wave generation using a soliton pulse within a nano-waveguide, IEEE Photon. Lett., 21(13), 932-934.

[9] Pornsuwancharoen N, Amiri IS, Suhailin FH, Aziz MS, Ali J, Singh G, Yupapin P.(2017), Micro-current source generated by a WGM of light within a stacked silicon-graphene-Au waveguide, IEEE Photon. Technol. Lett., 19, 1768-1771.

[10] Pornsuwancharoen N, Youplao P, Amiri IS, Ali J, Yupapin P (2017), Electron driven mobility model by light on the stacked metal-dielectric-interfaces, Microw. & Opti. Techn. Lett., 59, 1704-1709.

[11] Pornsuwancharoen, N., Youplao, P., Aziz, M.S., Ali, J., Singh, G., Amiri, I.S., Punthawanunt, S., Yupapin, P. 2018, Characteristics of microring circuit using plasmonic island driven electron mobility, Microsystem Technologies, 1-5.

[12] Pornsuwancharoen, N., Youplao, P., Aziz, M.S., Ali, J., Amiri, I.S., Punthawanunt, S., Yupapin, P. and Grattan, K.T.V. 2018, In-situ 3D micro-sensor model using embedded plasmonic island for biosensors, Microsystem and Technologies, In press.

[13] Basnayaka, A.D., and Hass, H. 2017, Aggregate signal interference of downlink LiFi networks, GLOBECOM 2017-2017 IEEE Global Communications Conference, 1-6.

[14] Wu, X. and Pass, H. 2017, Access point assignment in hybrid LiFi and WiFi networks in consideration of LiFi channel blockage, 2017 IEEE 18th International Workshop on Signal processing Advances in Wireless Communications(SPAWC), 1-5.

[15] Wang, Y., Basayaka, D.A., Wu, X. and Pass, H. 2017, Optimization of Load Balancing in Hybrid LiFi/RF networks, IEEE Transactions on Communications, 65(4), 1708-1702.

[16] Wu, X., Safari, M. and Hass, H. 2017, Joint optimization of load balancing and handover for hybrid LiFi and WiFi networks, 2017 IEEE Wireless Communications and networking Conference(WCNC), 1-5.

[17] Wang, Y., Wu, X. and Hass, H.2016, Analysis of area data rate with shadowing effects in Li-Fi and RF hybrid network, 2016 IEEE International Conference on Communications(ICC), 1-5.

[18] Zhou, L., You, H.-H. and Pu, X.-Y. 2011, Broadening free spectral range of an evanescent-wave pumped whispering-gallery-mode fiber fibre laser by Vernier effect, Optics Commun., 284(13), 3387-3390.
[19] Phatharacorn, P., Chiangga, S. and Yupapin, P. 2016, Analytical and simulation results of a triple micro whispering gallery mode probe system for a 3D blood flow rate sensor, Appl. Opt., 55(33), 009504.
[20] Phattharacorn, P., Chiangga, S., Ali, J. And Yupapin, P., 2018, Micro-optical probe model using integrated triple microring resonators for vertical depth identification, Microsystem and Technologies, In press.
[21] Pornsuwancharoen, N., Youplao, P., Aziz, M.S., Ali, J., Amiri, I.S., Punthawanunt, S., Yupapin, P. and K.T.V. Grattan, K.T.V. 2018, In-situ 3D micro-sensor model using embedded plasmonic island for biosensors, Microsystem Technologies, In press.
[22] Ali, J., Youplao, P., Pornsuwancharoen, P., Aziz, M.S.. Chiangga, S., Amiri, I.S., Punthawanunt, S., Singh, G. and Yupapin, P. 2018, On-chip remote charger model using plasmonic island circuit, Results in Physics, Accepted.
[23] Ali, J., Pornsuwancharoen, N., Youplao, P., Aziz, M.S., Chiangga, S., Jaglan, J., Amiri, I.S. and Yupapin, P. 2018, A novel plasmonic interferometry and the potential applications, Results in Physics, 2018; 8: 438.
[24] Al, J., Pornsuwancharoen, P., Youplao, P., Amiri, I.S., Chaiwong, K., Chiangga, S., Singh, G. and Yupapin, P. 2018, Coherent light squeezing states within a modified microring system, Results in Physics, Submitted.
[25] Arahira, S., Watanabe, K., Shinozaki, K. and Ogawa, Y. 1992, Successive excited-state absorption through a multistep process in highly Er3+-doped fiber pumped by a 1.48-μm laser diode, Optics Letters, 17(23), 1679-1781.
[26] Liu, M., Luo, A.-P., Yan, Y.-R., Hu, S., Liu, Y.-C., Cui, H., Luo, Z.-C., Xu, W.-C., 2016, Successive soliton explosions in an ultrafast fiber laser, Optics Letters 41(6), 1181-1184.
[27] Masuda, H., Kuwahara, S., Kawakami, H., Hirano, A., Miyamoto, Y., Mori, A. and Sakamoto, T. 2004, Ultra-wideband remotely-pumped EDF/DRA hybrid inline-repeater system using tellurite-based EDFs and 1500-nm pumping method, Technical Digest (CD) (Optical Society of America, 2004), paper OWB2.
[28] Gall, D. 2016, Electron mean free path in elemental metals, J Appl. Phys., 119, 085101.
[29] Baccarani, G. and Ostoja, P. 1975, Electron mobility empirically related to the phosphorus concentration in silicon, Solid State Electron., 18(6), 579-580.